Exact ordering of energy levels for one-dimensional interacting Fermi gases with SU(N) symmetry

Lei Pan,[1,2] Yanxia Liu,[1,3] Haiping Hu,[1,4] Yunbo Zhang,[3] and Shu Chen[1,2,5,*]

[1]*Beijing National Laboratory for Condensed Matter Physics, Institute of Physics, Chinese Academy of Sciences, Beijing 100190, China*

[2]*School of Physical Sciences, University of Chinese Academy of Sciences, Beijing 100049, China*

[3]*Institute of Theoretical Physics, Shanxi University, Taiyuan 030006, China*

[4]*Department of Physics, The University of Texas at Dallas, Richardson, Texas 75080, USA*

[5]*Collaborative Innovation Center of Quantum Matter, Beijing, China*

(Received 14 February 2017; published 23 August 2017)

Based on the exact solution of one-dimensional Fermi gas systems with SU(N) symmetry in a hard wall, we demonstrate that we are able to sort the ordering of the lowest-energy eigenvalues of states with all allowed permutation symmetries, which can be solely marked by certain quantum numbers in the Bethe ansatz equations. Our results give examples beyond the scope of the generalized Lieb-Mattis theorem, which can only compare the ordering of energy levels of states belonging to different symmetry classes if they are comparable according to the pouring principle. In the strongly interacting regime, we show that the ordering of energy levels can be determined by an effective spin-exchange model, and we extend our results to a nonuniform system trapped in a harmonic potential.

DOI: 10.1103/PhysRevB.96.075149

I. INTRODUCTION

The experimental progress in trapping and manipulating ultracold atomic systems has provided an ideal platform for studying novel phenomena that are not easily accessible in solid-state systems [1]. A typical example is that the ultracold fermion system with large hyperfine spin can possess high symmetries of SU(N) and exhibits exotic quantum magnetic properties fundamentally different from the large-spin solid-state systems, which usually have only $SU(2)$ symmetry. Large-spin alkaline and alkaline-earth fermion systems with SU(N) symmetry have already been realized experimentally in recent years [2–10]. The experimental progress in ultracold Fermi gases has stimulated a considerable number of theoretical studies, which unveiled the high SU(N) symmetry that can give rise to exotic properties in quantum magnetism and pairing superfluidity [11–14]. In particular, in the strongly interacting limit, recent studies have shown that one-dimensional (1D) multicomponent gases can be effectively described by spin-exchange models [15–29] and may be applied to study the quantum magnetism of a spin system with SU(N) symmetry [30–37].

For an interacting spin-1/2 Fermi system with $SU(2)$ symmetry, the ground state is the spin singlet state according to the well-known Lieb-Mattis theorem (LMT) [38], which indicates $E(S) < E(S')$ if $S < S'$ for a system composed of N electrons interacting by an arbitrary symmetric potential, where $E(S)$ is the lowest energy of states with total spin S. Such a theorem cannot be applied to the system with SU(N) symmetry as the energy levels can no longer be sorted by the total spin S. Nevertheless, for the high-symmetry SU(N) system, Lieb and Mattis proved a theorem (hereafter referred as LMT II) that if α can be poured in β, then $E(\alpha) > E(\beta)$, where α and β are two different symmetry classes and $E(\alpha)$ and $E(\beta)$ are the respective ground-state energies of the two classes [38]. Obviously, there exist some symmetry classes beyond LMT II where one class cannot be poured into another and thus one is not able to compare their energy levels directly. Recently, the LMT II for the trapped multicomponent mixtures was tested by studying the 1D strongly interacting few-body Fermi gases, showing that the ground state corresponds to the most symmetric configuration allowed by the imbalance among the components [39].

Although the LMT II generally can predict correctly the ground state for a high-symmetry multicomponent system, it is still not clear whether the ordering of energy levels can be solely sorted according to their symmetry classes, especially for those symmetry classes that are not comparable by the pouring principle [38]. In this work, we attempt to provide some clues to this question by studying the repulsively interacting 1D multicomponent Fermi gas with SU(N) symmetry confined in a hard-wall potential. The model can be solved exactly using the powerful Bethe ansatz (BA) method [40,41], permitting us to obtain the exact energy spectrum for all allowed permutation symmetry classes corresponding to various Young tableaus. In particular, in the strongly interacting limit, we show that the spin part is effectively described by an SU(N) spin-exchange model, and its coupling strength can be derived exactly from the expansion of the ground-state energy. Therefore, the ordering of energy levels can be determined by the effective spin-exchange model. We then generalize our study to a system trapped in a harmonic trap, which can be effectively described by an inhomogeneous spin-exchange model, and we find that the ordering of energy levels fulfills similar distributions to those in the exactly solvable case.

II. MODEL AND RESULTS

We consider the 1D n-component fermionic systems with SU(N) symmetry, which can be described by the following Hamiltonian:

$$H = \sum_{i}^{N}\left[-\frac{\hbar^2}{2m}\frac{\partial^2}{\partial x_i^2} + V(x_i)\right] + g\sum_{i<j}\delta(x_i - x_j). \quad (1)$$

*Author to whom all correspondence should be addressed: schen@iphy.ac.cn

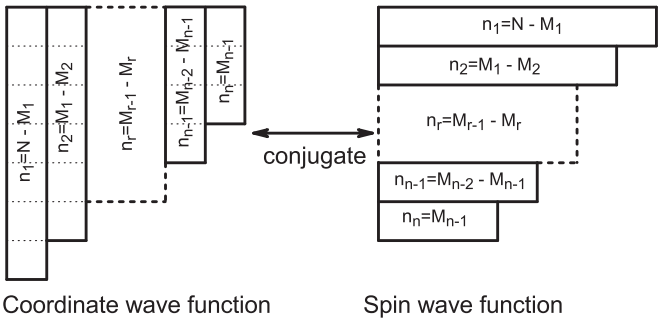

FIG. 1. Young tableau for the state of the $SU(N)$ N-particle system with given quantum numbers M_r. The left and right Young tableaus represent symmetry classes of the coordinate and spin wave functions, respectively, which are conjugated with each other.

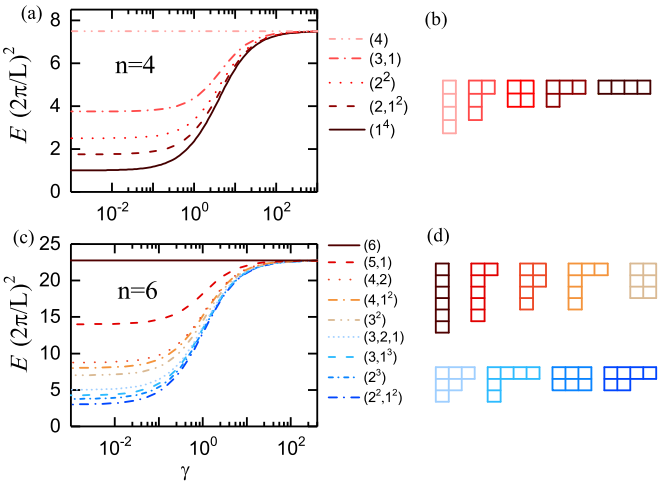

FIG. 2. Ground-state energies of states with different permutation symmetries vs the dimensionless interaction strength γ for the $SU(4)$ system with particle number (a) $N = 4$ and (c) $N = 6$. (a) Area from the dash-dot-dot line to the solid line corresponds to the lowest-energy states with different symmetry classes described by the Young tableaus of the coordinate wave function in (b). (c) Area from the solid line to the dash-dot line corresponds to different symmetry classes described by the Young tableaus shown in (d).

Here $V(x_i)$ is the external potential and g is the zero-range two-body interaction strength. The interactions between different components have the same coupling strength. For the spin-independent interactions, the particle number of each spin component is conserved. First we consider the exactly solvable case with $V(x_i) = 0$ for $x_i \in (-L/2, L/2)$ and otherwise $V = \infty$ under the open boundary condition $\Psi(x_i = \pm L/2) = 0$. For convenience, we introduce the interaction strength $c = mg/\hbar^2$ and use the natural units $\hbar^2 = 2m = 1$ in the following calculation. The system can be solved exactly using the BA method [40–42], and the corresponding Bethe ansatz equations (BAEs) are as follows:

$$2k_j L = 2\pi I_j - \sum_{\alpha=1}^{M_1}\left[\theta\left(\frac{k_j - \lambda_\alpha^1}{c/2}\right) + \theta\left(\frac{k_j + \lambda_\alpha^1}{c/2}\right)\right] \qquad (2)$$

with $j = 1,2,\ldots,N$ and

$$\sum_{\beta\neq\alpha}^{M_r}\left[\theta\left(\frac{\lambda_\alpha^r - \lambda_\beta^r}{c}\right) + \theta\left(\frac{\lambda_\alpha^r + \lambda_\beta^r}{c}\right)\right] = 2\pi J_\alpha^r + \sum_{\gamma=1}^{M_{r+1}}\left[\theta\left(\frac{\lambda_\alpha^r - \lambda_\gamma^{r+1}}{c/2}\right) + \theta\left(\frac{\lambda_\alpha^r + \lambda_\gamma^{r+1}}{c/2}\right)\right] + \sum_{\delta=1}^{M_{r-1}}\left[\theta\left(\frac{\lambda_\alpha^r - \lambda_\delta^{r-1}}{c/2}\right) + \theta\left(\frac{\lambda_\alpha^r + \lambda_\delta^{r-1}}{c/2}\right)\right], \qquad (3)$$

with $\alpha = 1,\ldots,M_r$ and $r = 1,2,\ldots,n-1$, where $\lambda_\delta^0 = k_\delta$, $\theta(x) = 2\arctan x$, $M_0 = N$, $M_n = 0$, and M_r takes integers in descending order, $M_0 > M_1 > \cdots > M_r$. The quantum numbers I_j and J_α^r are integers. $\boldsymbol{k_j}$'s are quasimomentum and λ_α^r denote the spin rapidities, which are introduced to describe the motion of spin waves. The particle number n_r in each spin component connects with M_r via the relation $n_r = M_{r-1} - M_r$, where we have assumed the components are ordered so that $n_1 \geqslant n_2 \geqslant \cdots \geqslant n_n$. For the repulsive case with $c > 0$, there is no charged bound state and the quasimomenta $\{k_j\}$ take real values. The eigenvalue is given by $E = \Sigma_{j=1}^N k_j^2$.

For a given set of $\{M_r\}$ $(r = 0,\ldots,n-1)$, there exists a unique Young tableau corresponding to the unique set of particle number distributions $\{n_r\}$ (see Fig. 1). Taking the case of $N = 4$ with $SU(4)$ symmetry as an example, $\{M_r\}$ $(r = 0,\ldots,3)$ can have five different configurations, i.e., $\{M_r\} = \{4,3,2,1\}$, $\{4,2,1,0\}$, $\{4,2,0,0\}$, $\{4,1,0,0\}$, and $\{4,0,0,0\}$. Correspondingly there exist five sets of $\{n_r\}$, say, $\{n_r\} = \{1,1,1,1\}$, $\{2,1,1\}$, $\{2,2\}$, $\{3,1\}$, and $\{4\}$, which belong to different symmetry classes with their eigenfunctions described by the Young tableaus in Fig. 2(b), denoted by the simplified notations $Y = (1,1,1,1) \equiv (1^4)$, $(2,1,1) \equiv (2,1^2)$, $(2,2) \equiv (2^2)$, $(3,1)$, and (4), from right to left, respectively. Here n_r $(r = 1,\ldots,4)$ in (n_1,n_2,n_3,n_4) indicates the number of squares in the rth column of the Young tableau, and the square numbers in the rth column are equal to the particle numbers n_r of the rth component. For example, $(1,1,1,1)$ describes the Young tableau □□□□, which corresponds to the system with the component-dependent particle numbers $n_1 = n_2 = n_3 = n_4 = 1$. We note that the notation adopted here is different from the standard notation of a representation of the Young tableau, but it is the same as that in Ref. [43].

According to the LMT II for the high-symmetry system, one can compare the ground-state energies of different symmetry classes if they fulfill the pouring principle. When we say that α can be poured in β, where the Young tableau α has the columns $n_1 \geqslant n_2 \geqslant n_3 \geqslant \cdots$ and β has the columns $n_1' \geqslant n_2' \geqslant n_3' \geqslant \cdots$, it means that we have $n_1 \geqslant n_1'$; $(n_1 - n_1') + n_2 \geqslant n_2'$; $(n_1 - n_1') + (n_2 - n_2') + n_3 \geqslant n_3'$; *et al.*, here any missing columns are to be regarded as having $n = 0$ [38]. Different from the $SU(2)$ system, for the $SU(N)$ system some symmetry classes are not comparable by the pouring principle, e.g., symmetry classes denoted by $(3,3)$ and $(4,1^2)$ for the $SU(4)$ system with $N = 6$.

Due to the unique correspondence between the symmetry classes and quantum numbers in the BAEs, we can calculate the lowest eigenenergy for each given symmetry class by numerically solving the corresponding BAEs with the quantum numbers $\{I_j\} = \{1,2,\ldots,N\}$ and $\{J_\alpha^r\} = \{1,2,\ldots,M_r\}$, which permits us to determine the order of energy levels with

different symmetries. We present our results for the spin-3/2 fermionic gas with $SU(4)$ symmetry in Fig. 2. For the case of $N = 4$ with five sets of $\{M_r\}$, the corresponding lowest energies for each symmetry class are shown in Fig. 2(a), indicating that the order of the energy levels fulfills $E(4) > E(3,1) > E(2,2) > E(2,1^2) > E(1^4)$ in the whole regime $0 \leqslant \gamma < \infty$ except in the Tonks-Girardeau limit, $\gamma \to \infty$, in which all the levels approach the same value, where $\gamma = cL/N$ is the dimensionless interaction strength. We note that in this case, the order of energy levels can also be determined by applying the LMT II, as all five symmetry classes are comparable according to the pouring principle. However, for the case of $N = 6$, there exist incomparable symmetry classes, as discussed before. Neither $(4,1^2)$ nor (3^2) can be poured into each other, so the LMT cannot determine the order of $E(4,1^2)$ and $E(3^2)$. Also, $E(3,1^3)$ and $E(2^3)$ are not comparable by the pouring principle. Similar to the case of $N = 4$, all the symmetry classes for $N = 6$ can be uniquely determined by solving the BAEs, and thus we can give an order of the energy levels as demonstrated in Fig. 2(c). From our calculated results, we can determine the order of energy levels of the incomparable symmetry classes, and we have $E(4,1^2) > E(3^2)$ and $E(3,1^3) > E(2^3)$. As shown in Fig. 2(c), the order of ground-state energies with different symmetries does not change for arbitrary finite interaction strength, and no phase transition occurs in the whole repulsive interaction region.

In the strongly repulsive regime ($cL/N \gg 1$), spin rapidities $\lambda_\alpha^{(r)}$ are proportional to c while k_j remains finite. From the expansion of Eq. (2) up to the first order in k_j/c, the quasimomentum is given by $2k_jL = 2\pi I_j - 2\zeta\frac{k_j}{c} + O(|c|^{-3})$, which leads to $k_j = \frac{\pi}{L}I_j(1 + \frac{1}{cL}\zeta)$ with

$$\zeta = \sum_{\alpha=1}^{M_1} \frac{4}{1 + 4\left(\gamma_\alpha^1\right)^2}. \tag{4}$$

Here $\gamma_\alpha^r \equiv \lambda_\alpha^r/c$, and γ_α^1 is determined by the following equation:

$$2N\theta\left(2\gamma_\alpha^1\right) = 2\pi J_\alpha^1 - \sum_{\beta\neq\alpha}^{M_1}\left[\theta\left(\gamma_\alpha^1 - \gamma_\beta^1\right) + \theta\left(\gamma_\alpha^1 + \gamma_\beta^1\right)\right] - \sum_{\gamma=1}^{M_2}\left[\theta\left(2\gamma_\alpha^1 - 2\gamma_\gamma^2\right) + \theta\left(2\gamma_\alpha^1 + 2\gamma_\gamma^2\right)\right], \tag{5}$$

which is obtained from the expansion of the second BAEs, i.e., Eq. (3) with $r = 1$, up to first order in k_j/c. The above equation cannot solely determine γ_α^1 as it includes γ_α^2, which should be iteratively determined by the following equations:

$$\sum_{\beta\neq\alpha}^{M_r}\left[\theta\left(\gamma_\alpha^r - \gamma_\beta^r\right) + \theta\left(\gamma_\alpha^r + \gamma_\beta^r\right)\right] = 2\pi J_\alpha^r + \sum_{\gamma=1}^{M_{r+1}}\left[\theta\left(2\gamma_\alpha^r - 2\gamma_\gamma^{r+1}\right) + \theta\left(2\gamma_\alpha^r + 2\gamma_\gamma^{r+1}\right)\right] + \sum_{\delta=1}^{M_{r-1}}\left[\theta\left(2\gamma_\alpha^r - 2\gamma_\delta^{r-1}\right) + \theta\left(2\gamma_\alpha^r + 2\gamma_\delta^{r-1}\right)\right], \tag{6}$$

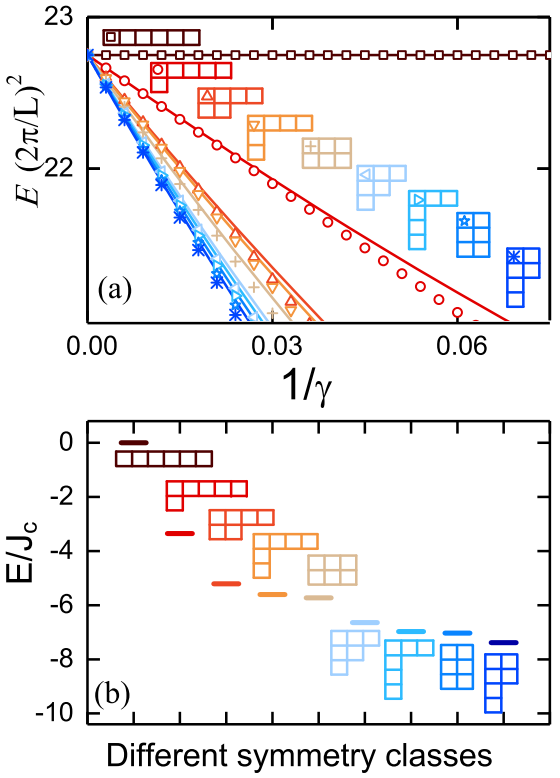

FIG. 3. (a) The lowest energy vs $1/\gamma$ for various symmetry classes. The scattered symbols represent results obtained from the effective spin chain, whereas the solid lines are obtained by solving the BAES. (b) The lowest energy calculated by exact diagonalization of the effective spin chain model of the $SU(4)$ system with $N = 6$ in a harmonic trap for various symmetry classes. Here we use the Young tableaus of the spin wave function, which conjugate with the tableaus of the coordinate wave function in Fig. 2(d), to represent different symmetry classes.

with $\alpha = 1, \ldots, M_r$ ($r = 2, \ldots n-1$). Up to the order of c^{-1}, the ground-state energy of the $SU(N)$ Fermi gas is given by

$$E = E_F\left(1 - \frac{2}{cL}\zeta\right) = E_F\left(1 - 2\frac{\zeta/N}{\gamma}\right), \tag{7}$$

where $E_F = \frac{\hbar^2\pi^2}{2mL^2}\frac{2N^3+3N^2+N}{6}$ is the energy at $c = \infty$. It is equal to the Fermi energy of fully polarized Fermi gas, consistent with that from the generalized Bose-Fermi mapping [42–47].

We note that Eqs. (5) and (6) are the well-known Bethe equations for the open $SU(N)$ Heisenberg spin chain

$$H_S = J\sum_{i=1}^{N-1}(P_{i,i+1} - 1), \tag{8}$$

where $P_{i,i+1}$ is the permutation operator, which permutes the spin states of the ith and $(i+1)$th particles. The ground-state energy of H_S with $J > 0$ is given by $E_S = -J\zeta$ [48]. By comparing with Eq. (7), we see that the effective Hamiltonian describing the spin dynamics in the strongly interacting limit is given by $H_{\text{eff}} = H - E_F = H_S$ with the exchange parameter given by $J = 2\frac{\epsilon_F}{\gamma}$, where $\epsilon_F = E_F/N$ is the average Fermi energy. In Fig. 3(a), we show the energy spectrum of H

in the strongly repulsive limit for the uniform system with $N = 6$ by using the effective Hamiltonian $H = E_F + H_S$. In the infinitely repulsive limit $\gamma \to \infty$, all the energy levels of different symmetry classes are degenerate. Since the ground-state energies of H_S for systems belonging to different symmetry classes take different values, the energy levels split when the interaction strength deviates from the TG limit. The order of the splitting levels can conveniently be distinguished by the Young diagrams of the spin wave function, which are the conjugations of the Young diagrams of the coordinate wave function (see Fig. 1).

In the strongly interacting regime, the $SU(\mathrm{N})$ Fermi gas in an inhomogeneous potential can also be described by a nonuniform effective spin-chain model,

$$H_{\mathrm{eff}} = \sum_{i=1}^{N-1} J_i (P_{i,i+1} - 1), \tag{9}$$

with the coefficients given by

$$J_i = \frac{2N!}{c} \int \prod_j dx_j |\partial_i \varphi_A|^2 \delta(x_i - x_{i+1}) \theta^1_{[i,i+1]},$$

where $\theta^1_{[i,i+1]} = \theta^1/\theta(x_i - x_{i+1})$ is a reduced sector function, θ^1 being the Heaviside step function whose value is 1 in the region $x_1 < x_2 < \cdots < x_N$ and zero otherwise [22,24]. The wave function φ_A is taken as the ground state of N spinless fermions, i.e., the Slater determinant made up of the lowest N level of eigenstates. The difference from the uniform system is that the exchange coefficients are site-dependent. A generalization of LMT for the $SU(\mathrm{N})$ chain is given in Ref. [49]. Consider the $SU(4)$ system with $N = 6$ in a harmonic trap $V(x) = m\omega^2 x^2/2$ with the trapping frequency ω. We get a nonuniform $SU(4)$ spin chain with $J_3 \equiv J_c$, $J_1 = J_5 = 0.5743 J_c$, and $J_2 = J_4 = 0.8956 J_c$, where J_c represents the effective exchange strength between two spins in the trap center. By directly diagonalizing the corresponding spin chain model, we can get the order of energy levels for the harmonic system in the strong interaction strength region. As shown in Fig. 3(b), the order of energy levels is solely related to their symmetry classes, which agrees with the case of a uniform system. Our result indicates that the order of energy levels in the strongly interacting regime is not changed when the trap potential is changed from the hard wall to the harmonic trap. Strongly interacting systems trapped in other external traps can also be studied similarly by solving the corresponding effective spin-exchange models.

Our results can be directly generalized to the multicomponent $SU(\mathrm{N})$ system with larger n, for example the system with $SU(6)$ symmetry, for which the BAEs take the form of Eqs. (2) and (3) with $n = 6$. For the example system with $N = 6$, by solving the corresponding BAEs, we can get the ground-state energies for 11 symmetry classes. The corresponding results are shown in Fig. 4. Compared to the case of $SU(4)$, there are two extra symmetry classes $(2,1^4)$ and (1^6), and similarly there also exist incomparable symmetry classes by the pouring principle, e.g., $(4,1^2)$ and (3^2), as well as $(3,1^3)$ and (2^3). The exact BA result gives the order of ground-state energy levels of different symmetry classes: $E(6) \geqslant E(5,1) \geqslant E(4,2) \geqslant \cdots \geqslant E(2,1^4) \geqslant E(1^6)$, where "=" holds true only in the TG limit $\gamma \to \infty$. As shown in Fig. 4, the order is unchanged in the whole interaction region.

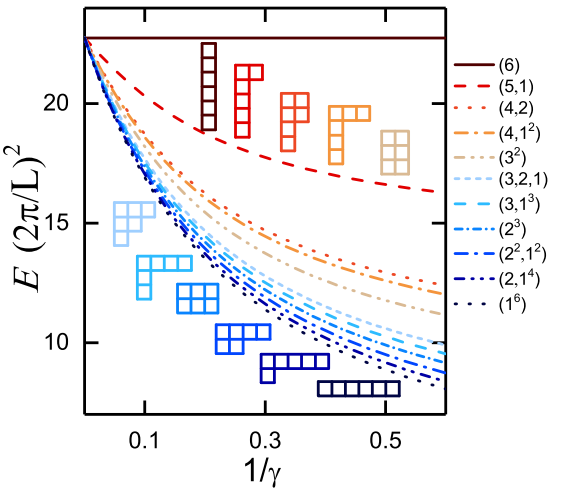

FIG. 4. The ground-state energies of 11 symmetry classes vs $1/\gamma$ for the $SU(6)$ system with $N = 6$. The area from the dark red solid line to the dark blue dotted line corresponds to the lowest-energy states of different symmetry classes described by the corresponding Young tableaus.

III. SUMMARY

In summary, based on the BA solution of few-particle systems, we have studied the ordering of energy levels for all kinds of permutation symmetry classes of 1D multicomponent Fermi systems with $SU(\mathrm{N})$ symmetry. In the strongly interacting regime, from the expansion of the BA solutions, we demonstrate that the system can be effectively described by an $SU(\mathrm{N})$ spin exchange model with the exchange parameter being exactly determined. Furthermore, the ordering of energy levels of the strongly interacting system trapped in a harmonic potential is also determined by solving its effective spin-exchange model.

ACKNOWLEDGMENTS

The work is supported by the National Key Research and Development Program of China (Grant No. 2016YFA0300600), NSFC under Grants No. 11425419, No. 11374354, and No. 11174360, and the Strategic Priority Research Program (B) of the Chinese Academy of Sciences (Grant No. XDB07020000). Y.Z. is supported by NSF of China under Grants No. 11474189 and No. 11674201.

L.P and Y.L. contributed equally to this work.

[1] I. Bloch, J. Dalibard, and W. Zwerger, Rev. Mod. Phys. **80**, 885 (2008).

[2] T. B. Ottenstein, T. Lompe, M. Kohnen, A. N. Wenz, and S. Jochim, Phys. Rev. Lett. **101**, 203202 (2008).

[3] J. H. Huckans, J. R. Williams, E. L. Hazlett, R. W. Stites, and K. M. O'Hara, Phys. Rev. Lett. **102**, 165302 (2009).

[4] X. Zhang, M. Bishof, S. L. Bromley, C. V. Kraus, M. S. Safronova, P. Zoller, A. M. Rey, and J. Ye, Science **345**, 1467 (2014).

[5] F. Scazza, C. Hofrichter, M. Höfer, P. C. De Groot, I. Bloch, S. Fölling, Nat. Phys. **10**, 779 (2014).

[6] G. Cappellini, M. Mancini, G. Pagano, P. Lombardi, L. Livi, M. Siciliani de Cumis, P. Cancio, M. Pizzocaro, D. Calonico, F. Levi, C. Sias, J. Catani, M. Inguscio, and L. Fallani, Phys. Rev. Lett. **113**, 120402 (2014).

[7] M. A. Cazalilla, A. F. Ho, and M. Ueda, New J. Phys. **11**, 103033 (2009).

[8] S. Taie, Y. Takasu, S. Sugawa, R. Yamazaki, T. Tsujimoto, R. Murakami, and Y. Takahashi, Phys. Rev. Lett. **105**, 190401 (2010).

[9] C. Hofrichter, L. Riegger, F. Scazza, M. Höfer, D. R. Fernandes, I. Bloch, and S. Fölling, Phys. Rev. X **6**, 021030 (2016).

[10] G. Pagano, M. Mancini, G. Cappellini, P. Lombardi, F. Schäfer, H. Hu, X.-J. Liu, J. Catani, C. Sias, M. Inguscio, and L. Fallani, Nat. Phys. **10**, 198 (2014).

[11] C. Wu, Phys. Rev. Lett. **95**, 266404 (2005); C. Wu, J. P. Hu, and S. C. Zhang, *ibid.* **91**, 186402 (2003).

[12] S. Chen, C. Wu, S. C. Zhang, and Y. Wang, Phys. Rev. B **72**, 214428 (2005).

[13] D. Wang, Y. Li, Z. Cai, Z. Zhou, Y. Wang, and C. Wu, Phys. Rev. Lett. **112**, 156403 (2014).

[14] P. Nataf and F. Mila, Phys. Rev. Lett. **113**, 127204 (2014).

[15] A. G. Volosniev, D. V. Fedorov, A. S. Jensen, M. Valiente, and N. T. Zinner, Nat. Commun. **5**, 5300 (2014).

[16] F. Deuretzbacher, D. Becker, J. Bjerlin, S. M. Reimann, and L. Santos, Phys. Rev. A **90**, 013611 (2014).

[17] A. G. Volosniev, D. Petrosyan, M. Valiente, D. V. Fedorov, A. S. Jensen, and N. T. Zinner, Phys. Rev. A **91**, 023620 (2015).

[18] J. Levinsen, P. Massignan, G. M. Bruun, and, M. M. Parish, Sci. Adv. **1**, e1500197 (2015).

[19] P. Massignan, J. Levinsen, and M. M. Parish, Phys. Rev. Lett. **115**, 247202 (2015).

[20] F. Deuretzbacher, D. Becker, and L. Santos, Phys. Rev. A **94**, 023606 (2016).

[21] F. Deuretzbacher, D. Becker, J. Bjerlin, S. M. Reimann, and L. Santos, Phys. Rev. A **95**, 043630 (2017).

[22] L. Yang, L. Guan, and H. Pu, Phys. Rev. A **91**, 043634 (2015).

[23] A. S. Dehkharghani, A. G. Volosniev, E. J. Lindgren, J. Rotureau, C. Forssn, D. V. Fedorov, A. S. Jensen, and N. T. Zinner, Sci. Rep. **5**, 16075 (2015).

[24] L. Yang and X. Cui, Phys. Rev. A **93**, 013617 (2016).

[25] H. Hu, L. Pan, and S. Chen, Phys. Rev. A **93**, 033636 (2016)

[26] L. Yang and H. Pu, Phys. Rev. A **94**, 033614 (2016).

[27] H. Hu, L. Guan, and S. Chen, New J. Phys. **18**, 025009 (2016).

[28] A. G. Volosniev, Few-Body Syst. **58**, 54 (2017).

[29] N. L. Harshman, Few-Body Syst. **57**, 45 (2016); **57**, 11 (2016).

[30] Z. Zhou, Z. Cai, C. Wu, and Y. Wang, Phys. Rev. B **90**, 235139 (2014).

[31] V. Bois, S. Capponi, P. Lecheminant, M. Moliner, and K. Totsuka, Phys. Rev. B **91**, 075121 (2015).

[32] B. Gertjerenken and M. Holthaus, Phys. Rev. A **90**, 053614 (2014).

[33] M. E. Beverland, G. Alagic, M. J. Martin, A. P. Koller, A. M. Rey, and A. V. Gorshkov, Phys. Rev. A **93**, 051601(R) (2016).

[34] P. Nataf, M. Lajkó, P. Corboz, A. M. Läuchli, K. Penc, and F. Mila, Phys. Rev. B **93**, 201113(R) (2016).

[35] P. Nataf and F. Mila, Phys. Rev. B **93**, 155134 (2016).

[36] X.-W. Guan, Z.-Q. Ma, and B. Wilson, Phys. Rev. A **85**, 033633 (2012); Y. Jiang, P. He, and X.-W. Guan, J. Phys. A **49**, 174005 (2016).

[37] S. Capponi, P. Lecheminant, and K. Totsuka, Ann. Phys. (NY) **367**, 50 (2016).

[38] E. Lieb and D. Mattis, Phys. Rev. **125**, 164 (1962).

[39] J. Decamp, P. Armagnat, B. Fang, M. Albert, A. Minguzzi, and P. Vignolo, New J. Phys. **18**, 055011 (2016).

[40] B. Sutherland, Phys. Rev. Lett. **20**, 98 (1968).

[41] M. Gaudin, Phys. Rev. A **4**, 386 (1971).

[42] N. Oelkers, M. T. Batchelor, M. Bortz, and X.-W. Guan, J. Phys. A **39**, 1073 (2006).

[43] C. N. Yang, Chin. Phys. Lett. **26**, 120504 (2009).

[44] M. D. Girardeau and A. Minguzzi, Phys. Rev. Lett. **99**, 230402 (2007).

[45] F. Deuretzbacher, K. Fredenhagen, D. Becker, K. Bongs, K. Sengstock, and D. Pfannkuche, Phys. Rev. Lett. **100**, 160405 (2008).

[46] L. Guan, S. Chen, Y. Wang, and Z. Q. Ma, Phys. Rev. Lett. **102**, 160402 (2009).

[47] M. D. Girardeau, J. Math. Phys. **1**, 516 (1960).

[48] B. Sutherland, Phys. Rev. B **12**, 3795 (1975).

[49] T. Hakobyan, Nucl. Phys. B **699**, 575 (2004); SIGMA **6**, 024 (2010).